RSC Advances

PAPER

View Article Online
View Journal | View Issue

Cite this: *RSC Adv.*, 2021, **11**, 33294

A highly selective quinolizinium-based fluorescent probe for cysteine detection†

Wa-Yi O,[ab] Wing-Cheung Chan,[b] Caifeng Xu,[a] Jie-Ren Deng,[b] Ben Chi-Bun Ko*[b] and Man-Kin Wong *[ab]

Received 12th August 2021
Accepted 24th September 2021

DOI: 10.1039/d1ra06104f

rsc.li/rsc-advances

A novel fluorescent quinolizinium-based turn-off probe has been developed for selective detection of cysteine. The probe showed high selectivity and sensitivity towards cysteine over other amino acids including the similarly structured homocysteine and glutathione with a detection limit of 0.18 μM (S/N = 3). It was successfully applied to cysteine detection in living cells with low cytotoxicity and quantitative analysis of spiked mouse serum samples with moderate to good recovery (96–109%).

Biothiols, including cysteine (Cys), homocysteine (Hcy) and glutathione (GSH), are biomolecules that play important roles in a variety of biological processes, such as cellular growth, redox homeostasis and immune system regulations.[1–5] Among the three biothiols, Cys is the essential amino acid involved in various physiological processes, in which it serves as a biomarker for different dysfunctions and diseases.[6] The deficiency of Cys can lead to adverse symptoms such as liver damage, psoriasis and lethargy, while high levels of Cys can cause a wide range of disorders such as Alzheimer's and cardiovascular diseases.[7–10] Therefore, it is of importance to develop effective and selective approaches for Cys detection under physiological conditions.

In the past decades, various techniques had been established for the detection of Cys, such as high performance liquid chromatography (HPLC),[11,12] capillary zone electrophoresis (CZE),[13–15] mass spectrometry (MS).[16,17] However, these methods require specialized equipment and sophisticated sample preparations, which restrict their applications on routine detection. In comparison, fluorescence spectroscopy is considered as a powerful technique for detection of Cys due to its high selectivity, operation simplicity, and non-invasiveness.[18–20] Nowadays, a variety of fluorescent probes have been developed based on the characteristic redox properties and strong nucleophilicity of the thiol group on Cys.[21–38] However, due to the structural similarity of Cys, Hcy and GSH, selective fluorescent detection of Cys in biological samples still remains a challenge.[39,40] Therefore, development of fluorescent probes for highly selective Cys detection is important.

Cys-triggered addition–cyclization–cleavage reaction with acrylate, which was first reported by Yang and Strongin in 2011,[41] is the most widely used response mechanism for the design of Cys-selective fluorescent probes.[5,18,20,21] Upon the addition of Cys, nucleophilic attack of Cys on acrylic ester followed by intramolecular cyclization releases the fluorophore's hydroxyl and a seven-membered ring amide. The high selectivity of this reaction towards Cys over Hcy and GSH is attributed to the kinetic difference of the intramolecular cyclization.

Various Cys-responsive fluorescent probes have been developed based on the incorporation of acrylate group on common fluorephores, such as BODIPY, rhodamine, coumarin and fluorescein.[42–50] However, the use of these dyes might suffer from low water solubility, which results in decreased sensitivity of detection and difficulty in biological applications.[22] In comparison, quinoliziniums are cationic aromatic heterocycles with improved water solubility, which enable their applications in cell imaging with good biocompatibility.[51,52] Compared with these common fluorescent scaffolds, studies on the applicability of quinolizinium compounds as fluorescent chemosensors remain largely elusive (Scheme 1).

In 2017, we have developed a new series of fluorescent quinolizinium compounds with tunable emission properties in visible light region (λ_{em} = 450 to 640 nm) and large Stokes shifts (up to 6797 cm^{-1}).[53] The application of this class of fluorescent quinoliziniums in live cell imaging was demonstrated by incubation with HeLa cells, in which the subcellular localization of the quinoliziniums could be switched by modifying the substituents. Based on this work, we envision that the fluorescent quinoliziniums would be amenable for the design of fluorescent probes for Cys detection in biological samples.

Herein we introduce a novel fluorescent quinolizinium-based turn-off probe **1** for highly selective detection of Cys over Hcy, GSH and other amino acids. The acrylate group was incorporated on the phenyl ring of the quinolizinium, which served as the moiety for the reaction with Cys. Cys triggered the

[a]*The Hong Kong Polytechnic University, Shenzhen Research Institute, Shenzhen, P. R. China. E-mail: mankin.wong@polyu.edu.hk*

[b]*State Key Laboratory of Chemical Biology and Drug Discovery, Department of Applied Biology and Chemical Technology, The Hong Kong Polytechnic University, Hung Hom, Hong Kong, P. R. China. E-mail: mankin.wong@polyu.edu.hk; ben.ko@polyu.edu.hk*

† Electronic supplementary information (ESI) available. See DOI: 10.1039/d1ra06104f

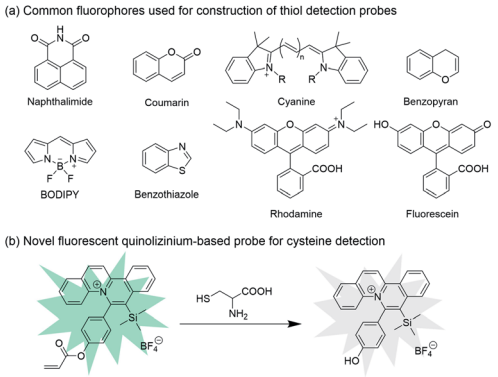

Scheme 1 (a) Common fluorophores used for construction of thiol detection probes. (b) Novel fluorescent quinolizinium-based probe for cysteine detection.

change in fluorescence intensity of probe **1** due to the conjugated addition–cyclization reaction with the acrylate group. The probe exhibited highly selective detection for Cys and good biocompatibility, which could be successfully applied to detection of Cys in living cells and quantitative analysis of Cys concentrations in mouse serum samples.

To verify the feasibility of probe **1** for Cys detection, the spectral properties of probe **1** towards Cys were firstly investigated in CH_3CN/H_2O solution (1 : 1, v/v, 50 mM pH 7.4 PBS). As shown in Fig. 1, the free probe **1** showed absorption bands at 360 nm and 420 nm. Upon excitation at 420 nm, strong fluorescent signal was observed at 495 nm. After the addition of Cys (20 equiv.), the absorption at 360 nm increased with the decreased absorption band at 420 nm, while the fluorescence intensity of probe **1** significantly reduced. These results indicated that probe **1** displayed fluorescence signal response towards Cys.

To examine the sensitivity of the probe, fluorescence titration of probe **1** (20 μM) was carried out in the presence of Cys in CH_3CN/H_2O solution (1 : 1, v/v, 50 mM pH 7.4 PBS) at 25 °C. The fluorescence quantum yield was evaluated to be 0.43 using coumarin 153 as a reference. Addition of 0.5 equiv. of Cys resulted in a decrease in fluorescence emission at 495 nm. The emission intensity was almost completely quenched upon addition of 20 equiv. of Cys, which showed a decrease in approximately 8-fold as compared with that of free probe **1**. Furthermore, probe **1** exhibited a good linear relationship between the emission intensities at 495 nm and the concentration of Cys ranging from 0 to 100 μM with a R^2 value of 0.9904 (Fig. 2b). The detection limit was evaluated to be 0.18 μM based on the equation LOD (Cys) = $3\sigma/m$, where σ is the standard deviation of blank measurements and m is the slope obtained from the calibration curve of probe **1** against Cys, indicating that probe **1** was highly sensitive to Cys.

We next investigated the selectivity of probe **1** for Cys. Under the same reaction conditions, other amino acids including Ala, Arg, Asn, Asp, Gln, Glu, Gly, His, Ile, Leu, Lys, Met, Phe, Pro, Ser, Thr, Trp, Tyr and Val caused almost no fluorescence intensity changes, which demonstrated the high selectivity of **1** to Cys over other amino acids even at high concentration (20 equiv., 400 μM). As shown in Fig. 3a, a distinct fluorescence ratio (F_0/F) induced by Cys could be observed in contrast to other amino acids, while Hcy and GSH showed only little effect to the fluorescence intensity changes. Besides, other potential biologically relevant cations and anions were investigated, including Na^+, K^+, Cu^+, Zn^{2+}, Cu^{2+}, Ni^{2+}, Mg^{2+}, Ca^{2+}, Fe^{3+}, Cl^-, Br^-, I^-, NO_3^-, SO_4^{2-}, HPO_4^-, $H_2PO_4^-$ and no significant fluorescence responses was observed (Fig. 3b).

To study the effect of pH to the fluorescence of probe **1**, the change in fluorescence emission intensity of probe **1** with and without Cys was investigated in a range of pH from 1 to 14, respectively. The fluorescence emission intensity of probe **1** at 495 nm was stable in the pH range of 6–9 (Fig. 4). Decrease in the fluorescence intensity was observed under basic conditions (pH > 9), which could be attributed to the hydrolysis of acrylate. The results suggested that probe **1** was capable of detecting Cys under physiological conditions.

The response time was examined based on the change in fluorescence emission intensity of probe **1** upon reaction with 20 equiv. of Cys, Hcy, and GSH, respectively. As shown in Fig. 5, Cys caused a rapid fluorescence quenching than Hcy and GSH, and the fluorescence intensity remained stable after 100 min. However, the reaction rates of Hcy and GSH with probe **1** were significantly lower than that of Cys. This result indicated that probe **1** could selectively distinguish Cys from Hcy and GSH.

Align with literature reports,[54–59] we proposed the reaction mechanism of probe **1** with Cys was based on the nucleophilic

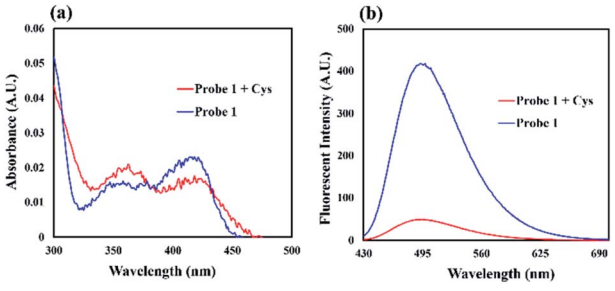

Fig. 1 (a) UV-Vis absorption and (b) fluorescence spectra of **1** (20 μM) with and without the addition of Cys (20 equiv.) in CH_3CN/H_2O solution (1 : 1, v/v, 50 mM pH 7.4 PBS) after 100 min.

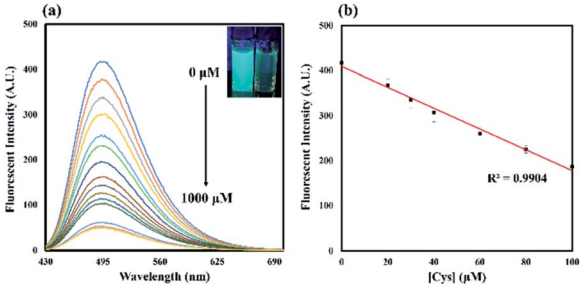

Fig. 2 (a) Fluorescence titration of **1** (20 μM) upon the addition of Cys (0, 10, 20, 30, 40, 60, 80, 100, 120, 140, 160, 180, 200, 400, 600, 1000 μM). (b) Linear correlation between emission intensities at 495 nm and concentrations of Cys (0–100 μM).

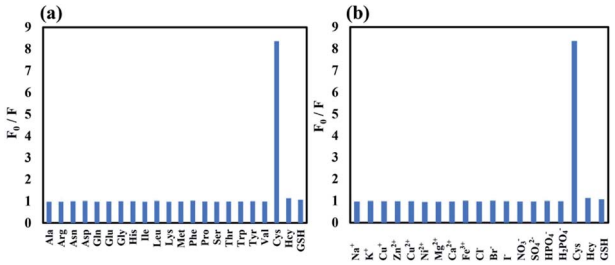

Fig. 3 Fluorescence changes F_0/F (λ_{em} = 495 nm) of **1** (20 μM) upon the addition of various (a) amino acids (20 equiv.) and (b) potential biologically-relevant ions in CH_3CN/H_2O solution (1 : 1, v/v, 50 mM pH 7.4 PBS) after 100 min.

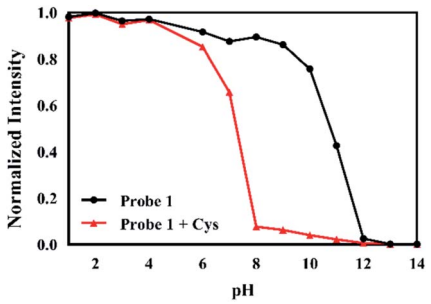

Fig. 4 Fluorescence intensity of **1** (20 μM) with and without the addition of Cys (20 equiv.) at different pH values.

addition reaction of Cys with C=C bond of acrylate, followed by the cyclization–cleavage reaction and resulting in the formation of **2** with a hydroxyl group (Scheme 2). HRMS analysis of the crude reaction mixture showed the presence of peak with *m*/*z* 394.16, which revealed the formation of **2** after the reaction (Fig. S2†). The high selectivity of probe **1** towards Cys over Hcy and GSH could be attributed to the difference in reaction rates of the intramolecular cyclization reaction. The intramolecular cyclization reaction for the formation of the seven-membered amide promoted by Cys was more kinetically favored than the formation of a strained eight or twelve-membered ring in the case of Hcy or GSH, respectively. As shown in the MS spectra

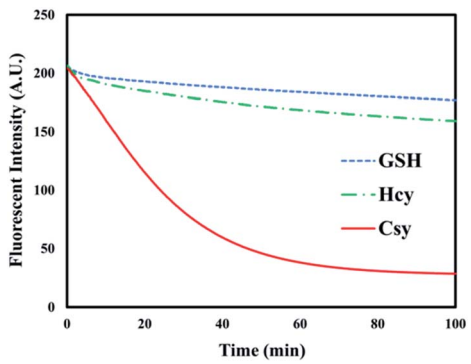

Fig. 5 Time-dependent fluorescence changes of **1** (20 μM) upon the addition of Cys, Hcy, and GSH (20 equiv.).

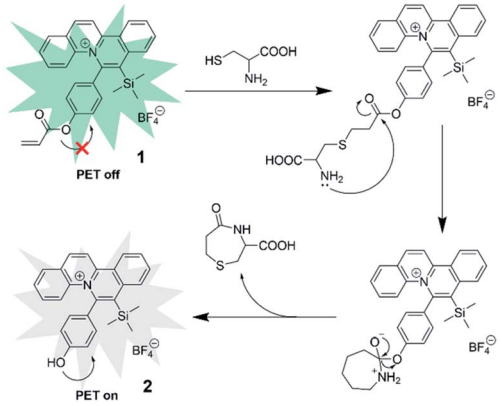

Scheme 2 Proposed reaction mechanism of **1** with Cys.

(Fig. S3 and S4†), the presence of peaks corresponding to the reaction intermediates, *m*/*z* 583.21 for Hcy and *m*/*z* 755.26 for GSH, respectively, was observed. These results indicated that Hcy and GSH exhibited slower reaction rates with probe **1**.

NMR analysis of the crude reaction mixture of probe **1** with Cys (3 equiv.) was performed to provide further evidence on this reaction mechanism. As shown in Fig. 6, the hydrogen atoms on the acrylate group were located at 6.12 ppm (1H), 6.40 ppm (1H) and 6.60 ppm (1H). After reaction with Cys, the peaks corresponding to the hydrogen atoms on the acrylate group disappeared, while the shift of two peaks at 7.28 ppm (2H) and 7.51 ppm (2H) to 6.90 ppm (2H) and 7.27 ppm (2H), respectively, which corresponding to the hydrogen atoms on the phenyl ring, was observed. By comparing the NMR spectrum of isolated **2** with that of the crude reaction mixture, the result indicated that Cys reacted with the acrylate group on probe **1**, resulting in the formation of **2** with the hydroxyl group.

The fluorescence was proposed to be quenched by the presence of hydroxyl substituent on the phenyl ring (*i.e.* phenol

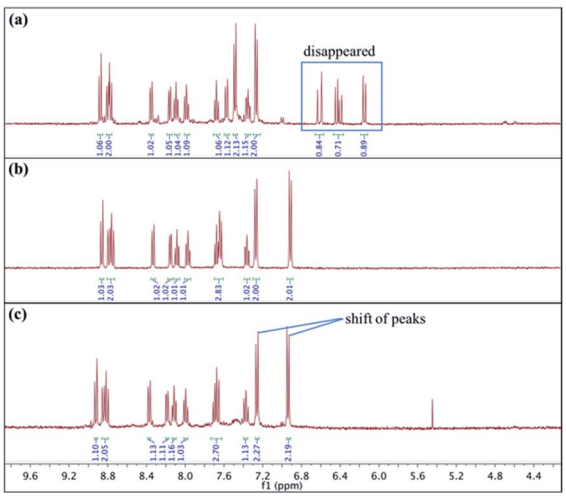

Fig. 6 Study of reaction mechanism using ^{1}H NMR analysis. (a) ^{1}H NMR spectrum of isolated **1**; (b) ^{1}H NMR spectrum of isolated **2**; (c) ^{1}H NMR spectrum of crude reaction mixture of **1** with Cys.

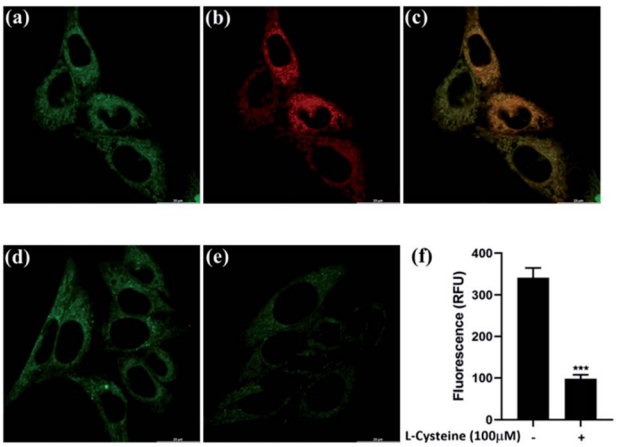

Fig. 7 Confocal fluorescence microscopic images of HeLa cells. (a) Subcellular localization of **1**. (b) Subcellular localization of MitoTracker™ Red FM. (c) Merged images of (a) and (b). (d) Control experiment of **1**-treated cells; (e) **1**-treated cells incubated with Cys (100 μM). (f) Relative fluorescence of cells measured by ImageJ.

moiety) of the quinolizinium *via* intramolecular photo-induced electron transfer (PET). According to our previous study on the structure–photophysical property relationship (SPPR) studies of the quinolizinium compounds, the HOMO is composed of a π orbital of the quinolizinium and phenyl ring while the LUMO is composed of a π* orbital of the quinolizinium ring. The O atom of the phenol moiety served as an electron-donating group that donated an electron from its HOMO to the half-filled HOMO of the quinolizinium upon excitation by light, resulting in the quenching of fluorescence.

To demonstrate the practical applicability of probe **1** in biological systems, cytotoxicity test and cell imaging experiments were carried out. HeLa cell lines (American Type Culture Collection) were cultured with Dulbecco's Modified Eagle's Medium (DMEM) (Gibco) supplemented with 44 mM sodium bicarbonate (Sigma-Aldrich), 10% v/v fetal bovine serum (Gibco), and 100 U mL^{-1} penicillin (Gibco), 100 μg mL^{-1} streptomycin (Gibco) at 37 °C with 5% CO_2. The cells had over 50% cell viability for concentrations of probe **1** up to 20.51 μM, revealing that probe **1** is of low toxicity and good biocompatibility. The colocalization images of HeLa cells were observed after treating with probe **1** and MitoTracker™ Red FM. As shown in Fig. 7c, the green fluorescence from probe **1** overlaid well with the red fluorescence from MitoTracker™ Red FM, indicating that probe **1** could specifically localized in the mitochondria.

For Cys detection in living cells, HeLa cells were first treated with 100 μM of L-cysteine for 30 min, followed by incubation with probe **1** for 2 h. L-Cysteine was replaced by PBS as the control experiment. The fluorescence imaging was conducted with a confocal microscope Leica TCS SP8 MP (Fig. 7d and e). Green fluorescence emission was observed for the control experiment, which possibly revealed that the interfering effects of other intracellular thiol-containing molecules, including Hcy, GSH and H_2S, should be negligible. The fluorescence emission was quenched by the presence of Cys in cells. These results demonstrated that probe **1** could detect Cys in living cells with mitochondrial targeting capability.

Table 1 Determination of Cys in mouse serum samples

	Cys concentration (μM)			
Sample	Spiked	Found	Recovery (%)	RSD (%) ($n = 4$)
Mouse serum	0	57.92	—	4.8
	20	76.70	108.9	2.9
	30	86.74	96.0	6.7
	40	101.68	109.4	1.4

We further explored the application of probe **1** in quantitative analysis of biological samples. Probe **1** was applied to the detection of Cys in mouse serum samples with literature references.[60–62] The serum samples were obtained from C57BL/6 mouse (source from The Chinese University of Hong Kong). Whole blood collected was allowed to clot by leaving it undisturbed for an hour at room temperature. The clotted blood was centrifuged at 1000 g for 10 min to remove the clot. Sera were separated and stored at −80 °C prior to the assay. The standard addition method was used to detect Cys in mouse serum. Mouse serum samples were diluted 1000-fold with PBS and Cys at different concentrations were added to the samples, respectively. After the reaction was incubated with probe **1** at 25 °C for 100 min, the fluorescence signals of samples were measured. The Cys concentration of each spiked sample was calculated from the linear calibration curve (Fig. S8†). As shown in Table 1, moderate to good recovery percentage was obtained in the range from 96% to 109%. These results indicated the possibility of probe **1** for the application in quantitative Cys determination in biological samples.

Conclusions

In summary, we have developed a novel fluorescent quinolizinium-based turn-off probe for highly selective detection of Cys. The acrylate group was incorporated on the phenyl ring of the quinolizinium, which served as the reaction site for conjugated addition–cyclization reaction with Cys, resulting in the formation of phenol moiety with fluorescence quenching *via* PET. Probe **1** exhibited high selectivity and sensitivity towards Cys over Hcy, GSH and other amino acids with a low detection limit of 0.18 μM. It was successfully applied to the detection of Cys in living cells with low cytotoxicity and good biocompatibility, as well as the quantitative analysis of spiked mouse serum samples with moderate to good recovery (96–109%).

Ethical statement

All animal procedures were performed in accordance with the Guidelines for Care and Use of Laboratory Animals of The Hong Kong Polytechnic University and experiments were approved by

the Animal Ethics Committee of The Hong Kong Polytechnic University (20-21/9-ABCT-R-OTHERS).

Conflicts of interest

M.-K. Wong, B. C.-B.-Ko, W.-Y. O, W.-C. Chan and J.-R. Deng applied patent on the approach of cysteine detection using quinolizinium-based fluorescent probes.

Acknowledgements

We gratefully acknowledge the financial support by the Shenzhen Science and Technology Innovation Commission (JCYJ20170818104257975), the State Key Laboratory of Chemical Biology and Drug Discovery, and The Hong Kong Polytechnic University (G-ZVQZ).

Notes and references

1 X. Chen, Y. Zhou, X. Peng and J. Yoon, *Chem. Soc. Rev.*, 2010, **39**, 2120–2135.
2 L. B. Poole, *Free Radic. Biol. Med.*, 2015, **80**, 148–157.
3 D. Trachootham, W. Q. Lu, M. A. Ogasawara, N. R. D. Valle and P. Huang, *Antioxid. Redox Signal.*, 2008, **10**, 1343–1374.
4 M. Benhar, *Antioxidants*, 2020, **9**, 309.
5 R. Zhang, J. Yong, J. Yuan and Z. P. Xu, *Coord. Chem. Rev.*, 2020, **408**, 213182.
6 J. Dai, C. Ma, P. Zhang, Y. Fu and B. Shen, *Dye. Pigment.*, 2020, **177**, 108321.
7 C. E. Paulsen and K. S. Carroll, *Chem. Rev.*, 2013, **113**, 4633–4679.
8 E. Weerapana, C. Wang, G. M. Simon, F. Richter, S. Khare, M. B. D. Dillon, D. A. Bachovchin, K. Mowen, D. Baker and B. F. Cravatt, *Nature*, 2010, **468**, 790–795.
9 Y. M. Go and D. P. Jones, *Free Radic. Biol. Med.*, 2011, **50**, 495–509.
10 A. Pastore, A. Alisi, G. di Giovamberardino, A. Crudele, S. Ceccarelli, N. Panera, C. Dionisi-Vici and V. Nobili, *Int. J. Mol. Sci.*, 2014, **15**, 21202–21214.
11 Y. V. Tcherkas and A. D. Denisenko, *J. Chromatogr. A*, 2001, **913**, 309–313.
12 W. Chen, Y. Zhao, T. Seefeldt and X. Guan, *J. Pharm. Biomed. Anal.*, 2008, **48**, 1375–1380.
13 G. Chen, L. Zhang and J. Wang, *Talanta*, 2004, **64**, 1018–1023.
14 P. Kubalczyk, E. Bald, P. Furmaniak and R. Głowacki, *Anal. Methods*, 2014, **6**, 4138–4143.
15 A. V. Ivanov, E. D. Virus, B. P. Luzyanin and A. A. Kubatiev, *J. Chromatogr. B*, 2015, **1004**, 30–36.
16 N. Burford, M. D. Eelman, D. E. Mahonyb and M. Morash, *Chem. Commun.*, 2003, 146–147.
17 G. Weaving, B. F. Rocks, S. A. Iversen and M. A. Titheradge, *Ann. Clin. Biochem.*, 2006, **43**, 474–480.
18 L.-Y. Niu, Y.-Z. Chen, H.-R. Zheng, L.-Z. Wu, C.-H. Tung and Q.-Z. Yang, *Chem. Soc. Rev.*, 2015, **44**, 6143–6160.
19 G. Sivaramana, M. Iniya, T. Anande, N. G. Kotlac, O. Sunnapu, S. Singaravadivel, A. Gulyani and D. Chellappa, *Coord. Chem. Rev.*, 2018, **357**, 50–104.
20 X. Chen, Y. Zhou, X. Peng and J. Yoon, *Chem. Soc. Rev.*, 2010, **39**, 2120–2135.
21 H. S. Jung, X. Chen, J. S. Kim and J. Yoon, *Chem. Soc. Rev.*, 2013, **42**, 6019–6031.
22 S. Wang, Y. Huang and X. Guan, *Molecules*, 2021, **26**, 3575.
23 H.-Y. Shiu, M.-K. Wong and C.-M. Che, *Chem. Commun.*, 2011, **47**, 4367–4369.
24 T. Anand, G. Sivaraman and D. Chellappa, *J. Photochem. Photobiol., A*, 2014, **281**, 47–52.
25 T. Anand, G. Sivaraman and D. Chellappa, *Spectrochim. Acta, Part A*, 2014, **123**, 18–24.
26 X. Dai, Z.-Y. Wang, Z.-F. Du, J. Cui, J.-Y. Miao and B.-X. Zhao, *Anal. Chim. Acta*, 2015, **900**, 103–110.
27 F. Ali, H. Anila, N. Taye, R. G. Gonnade, S. Chattopadhyay and A. Das, *Chem. Commun.*, 2015, **51**, 16932–16935.
28 K. Yin, F. Yu, W. Zhang and L. Chen, *Biosens. Bioelectron.*, 2015, **74**, 156–164.
29 L. He, X. Yang, K. Xu, X. Kong and W. Lin, *Chem. Sci.*, 2017, **8**, 6257–6265.
30 S. O. Raja, G. Sivaraman, A. Mukherjee, D. Chellappa and A. Gulyani, *ChemistrySelect*, 2017, **2**, 4609–4616.
31 H. Zhang, L. Xu, W. Chen, J. Huang, C. Huang, J. Sheng and X. Song, *ACS Sens*, 2018, **3**, 2513–2517.
32 M. Yang, J. Fan, W. Sun, J. Du and X. Peng, *Anal. Chem.*, 2019, **91**, 12531–12537.
33 J. Gao, Y. Tao, J. Zhang, N. Wang, X. Ji, J. He, Y. Si and W. Zhao, *Chem. - Eur. J.*, 2019, **25**, 11246–11256.
34 X. Lin, Y. Hu, D. Yang and B. Chen, *Dye. Pigment.*, 2020, **174**, 107956.
35 L. Wang, J. Wang, S. Xia, X. Wang, Y. Yu, H. Zhou and H. Liu, *Talanta*, 2020, **219**, 121296.
36 X. Ji, N. Wang, J. Zhang, S. Xu, Y. Si and W. Zhao, *Dye. Pigment.*, 2021, **187**, 109089.
37 S. O. Raja, G. Sivaraman, S. Biswas, G. Singh, F. Kalim, P. Kandaswamy and A. Gulyani, *ACS Appl. Bio Mater.*, 2021, **4**, 4361–4372.
38 X. Yue, J. Chen, W. Chen, B. Wang, H. Zhang and X. Song, *Spectrochim. Acta, Part A*, 2021, **250**, 119347.
39 C. Yin, F. Huo, J. Zhang, R. Martinez-Manez, Y. Yang and H. Lv, *Chem. Soc. Rev.*, 2013, **42**, 6032–6059.
40 C.-X. Yin, K.-M. Xiong, F.-J. Huo, J. C. Salamanca and R. M. Strongin, *Angew. Chem., Int. Ed.*, 2017, **56**, 13188–13198.
41 X. Yang, Y. Guo and R. M. Strongin, *Angew. Chem., Int. Ed.*, 2011, **50**, 10690–10693.
42 X. Dai, Q. H. Wu, P. C. Wang, J. Tian, Y. Xu, S. Q. Wang, J. Y. Miao and B. X. Zhao, *Biosens. Bioelectron.*, 2014, **59**, 35–39.
43 W.-W. Ma, M.-Y. Wang, D. Yin and X. Zhang, *Sens. Actuators B Chem.*, 2017, **248**, 332–337.
44 W. Fan, X. Huang, X. Shi, Z. Wang, Z. Lu, C. Fan and Q. Bo, *Spectrochim. Acta, Part A*, 2017, **173**, 918–923.

45 L. Pang, Y. Zhou, W. Gao, J. Zhang, H. Song, X. Wang, Y. Wang and X. Peng, *Ind. Eng. Chem. Res.*, 2017, **56**, 7650–7655.
46 Y.-J. Fu, Z. Li, C.-Y. Li, Y.-F. Li, P. Wu and Z.-H. Wen, *Dyes Pigm.*, 2017, **139**, 381–387.
47 X. Song, B. Dong, X. Kong, C. Wang, N. Zhang and W. Lin, *Anal. Methods*, 2017, **9**, 1891–1896.
48 B. Liang, B. Wang, Q. Ma, C. Xie, X. Li and S. Wang, *Spectrochim. Acta, Part A*, 2018, **192**, 67–74.
49 D. Chen, Z. Long, Y. Dang and Li Chen, *Dyes Pigm.*, 2019, **166**, 266–271.
50 X. Pei, F. Huo, Y. Yue, T. Chen and C. Yin, *Sens. Actuators B Chem.*, 2020, **304**, 127431.
51 Z. Xu and L. Xu, *Chem. Commun.*, 2016, **52**, 1094–1119.
52 P. Gao, W. Pan, N. Li and B. Tang, *Chem. Sci.*, 2019, **10**, 6035–6071.
53 J.-R. Deng, W.-C. Chan, N. C.-H. Lai, B. Yang, C.-S. Tsang, B. C.-B. Ko, S. L.-F. Chan and M.-K. Wong, *Chem. Sci.*, 2017, **8**, 7537–7544.
54 B. Liu, J. Wang, G. Zhang, R. Bai and Y. Pang, *ACS Appl. Mater. Interfaces*, 2014, **6**, 4402–4407.
55 P. Wang, Q. Wang, J. Huang, N. Li and Y. Gu, *Biosens. Bioelectron.*, 2017, **92**, 583–588.
56 M. Zhu, L. Wang, X. Wu, R. Na, Y. Wang, Q. X. Li and B. D. Hammock, *Anal. Chim. Acta*, 2019, **1058**, 155–165.
57 Y. Ji, F. Dai and B. Zhou, *Talanta*, 2019, **197**, 631–637.
58 T. Chen, X. Pei, Y. Yue, F. Huo and C. Yin, *Spectrochim. Acta, Part A*, 2019, **209**, 223–227.
59 Q. Liu, C. Liu, X. Jiao, S. Cai, S. He, L. Zhao, X. Zeng and T. Wang, *Dye. Pigment.*, 2021, **190**, 109293.
60 Z. Huang, C. Wu, Y. Li, Z. Zhou, R. Xie, X. Pang, H. Xu, H. Li and Y. Zhang, *Anal. Methods*, 2019, **11**, 3280–3285.
61 D. Rohilla, S. Chaudhary, N. Kaur and A. Shanavas, *Mater. Sci. Eng. C*, 2020, **110**, 110724.
62 G. Kalaiyarasan, C. Hemlata and J. Joseph, *ACS Omega*, 2019, **4**, 1007–1014.